

Search for the Standard Model Scalar Boson with the ATLAS detector

Sandra Kortner on behalf of the ATLAS Collaboration

Max-Planck-Institut für Physik, Föhringer Ring 6, D-80805 Munich, Germany

The experimental results of the search for the Standard Model Higgs boson with the ATLAS detector at the Large Hadron Collider are reported, based on a dataset of pp collision data with an integrated luminosity of up to 4.9 fb^{-1} at $\sqrt{s} = 7 \text{ TeV}$. The search combines several Higgs boson decay channels in a wide range of Higgs boson masses from 110 GeV to 600 GeV. A Standard Model Higgs boson is excluded at the 95% confidence level in the mass ranges from 110.0 GeV to 117.5 GeV, 118.5 GeV to 122.5 GeV, and 129 GeV to 539 GeV, while the range from 120 GeV to 555 GeV is expected to be excluded in the absence of a signal. The most significant excess of events is observed around 126 GeV with a local significance of 2.5σ . The global probability for such an excess to occur in the full searched mass range is approximately 30%.

1 Introduction

One of the main missing pieces of puzzle in the Standard Model (SM) of particle physics relates to the electroweak symmetry breaking mechanism [1,2,3,4] which predicts the existence of a new, yet undiscovered scalar boson, the Higgs boson. Electroweak precision measurements at the LEP, SLD and Tevatron experiments [5] set an indirect upper limit on the Higgs boson mass of $m_H < 152 \text{ GeV}$ at the 95% confidence level (CL). The existence of a Higgs boson in the mass regions with $m_H < 114.4 \text{ GeV}$ and $156 \text{ GeV} < m_H < 177 \text{ GeV}$ is excluded at the 95% CL by the LEP [6] and Tevatron [7] experiments, respectively. In the following, the latest results from direct searches for the SM Higgs boson with the ATLAS detector at the Large Hadron Collider (LHC) are presented. The results supersede the ones published in Ref.[8] and are based on the full dataset of pp collision data recorded in 2011 with an integrated luminosity of up to 4.9 fb^{-1} at a center-of-mass energy of $\sqrt{s}=7 \text{ TeV}$.

2 Search overview

The search for the SM Higgs boson is performed in the mass range from 110 GeV to 600 GeV combining several search channels summarized in Table 1. The Higgs boson decays into vector boson pairs allow for the search in the entire mass range, while the $H \rightarrow \gamma\gamma$, $H \rightarrow \tau^+\tau^-$ and $H \rightarrow b\bar{b}$ decay modes provide an additional sensitivity for a low-mass Higgs boson ($m_H < 150 \text{ GeV}$). As opposed to other channels, the $H \rightarrow \gamma\gamma$ and $H \rightarrow ZZ \rightarrow 4\ell$ decay modes are distinguished through their high signal mass resolution. Each search channel is divided into several exclusive sub-channels with different background composition or signal-to-background ratios. The exclusion limits on the Higgs boson production cross section are set based on the mass spectra of the final decay products, using the modified frequentist approach (CL_S) [17]. The p_0 -value, i.e. the probability that the expected background fluctuates as high as the observed number

Table 1: Individual channels in search for the SM Higgs boson along with the corresponding number of sub-channels, explored range of Higgs boson masses, integrated luminosity and references to public documentation.

Search channel	Nr. of subchannels	m_H range (GeV)	L (fb ⁻¹)	Reference
$H \rightarrow \gamma\gamma$	9	110-150	4.9	[9]
$H \rightarrow \tau\tau$	12	110-150	4.7	[10]
$VH, H \rightarrow bb$	11	110-130	4.7	[11]
$H \rightarrow WW^{(*)} \rightarrow \ell\nu\ell\nu$	9	110-600	4.7	[12]
$H \rightarrow ZZ^{(*)} \rightarrow 4\ell$	4	110-600	4.8	[13]
$H \rightarrow ZZ \rightarrow \ell\nu\nu$	4	200-600	4.7	[14]
$H \rightarrow ZZ \rightarrow \ell\ell jj$	2	200-600	4.7	[15]
$H \rightarrow WW \rightarrow \ell\nu jj$	4	300-600	4.7	[16]

of events or higher, has been evaluated for each hypothesized mass m_H using a frequentist approach [18]. The Higgs boson production cross sections and decay branching ratios, as well as the corresponding theory uncertainties are taken into account and are summarized in Ref. [19]. The QCD scale uncertainties depend on the mass m_H and typically amount to ${}^{+12}_{-8}\%$ for the dominant gluon fusion (ggH) production mode, $\pm 1\%$ for the production via vector boson fusion (VBF) and in association with vector bosons (VH), and ${}^{+3}_{-9}\%$ for the associated production with top-quark pairs ($t\bar{t}H$). The uncertainties related to the parton distribution functions (PDF) amount to $\pm 8\%$ for the predominantly gluon-initiated ggH and $t\bar{t}H$ processes, and $\pm 4\%$ for the predominantly quark-initiated VBF and VH processes.

3 Searches in the low- m_H region (110 GeV - 150 GeV)

3.1 $H \rightarrow \gamma\gamma$

Despite of a very small branching ratio of about 0.2%, the $H \rightarrow \gamma\gamma$ decay channel provides the highest sensitivity for the Higgs boson search in the mass region $m_H \lesssim 120$ GeV. Selection of two isolated photons with high transverse energy has been optimized for the suppression of the reducible photon-jet and jet-jet backgrounds with one or two misidentified jets. The irreducible background with true diphoton events comprises about 70% of all selected events in the explored mass range from 100 GeV to 150 GeV. The analysis is divided into 9 sub-categories based on the photon pseudorapidity, conversion status and $p_{Tt}^{\gamma\gamma}$, i.e. the component of the diphoton p_T orthogonal to the di-photon thrust axis. Excellent diphoton invariant mass resolution of 1% to 2% allows for the search of a narrow di-photon invariant mass peak from the Higgs boson decays on the continuum background. The inclusive invariant diphoton mass spectrum is shown in Figure 1 (left) together with the total expected background contribution. The background contributions are estimated separately in each sub-category from the fit of an exponential function to the diphoton invariant mass spectrum, while the signal shape is modelled by the sum of a Crystal Ball and a Gaussian function. The observed and expected exclusion limits at the 95% CL on the Higgs boson production in units of the SM cross section are shown in Figure 1 (right). A SM Higgs boson is excluded at the 95% CL in the mass ranges of 113 GeV-115 GeV and 134.5 GeV-136 GeV. The largest excess with respect to the background-only hypothesis is observed at 126.5 GeV with a local significance of 2.8σ . The corresponding global significance is 1.5σ after accounting for the look-elsewhere-effect (LEE) [20] in the entire mass range explored with this decay channel.

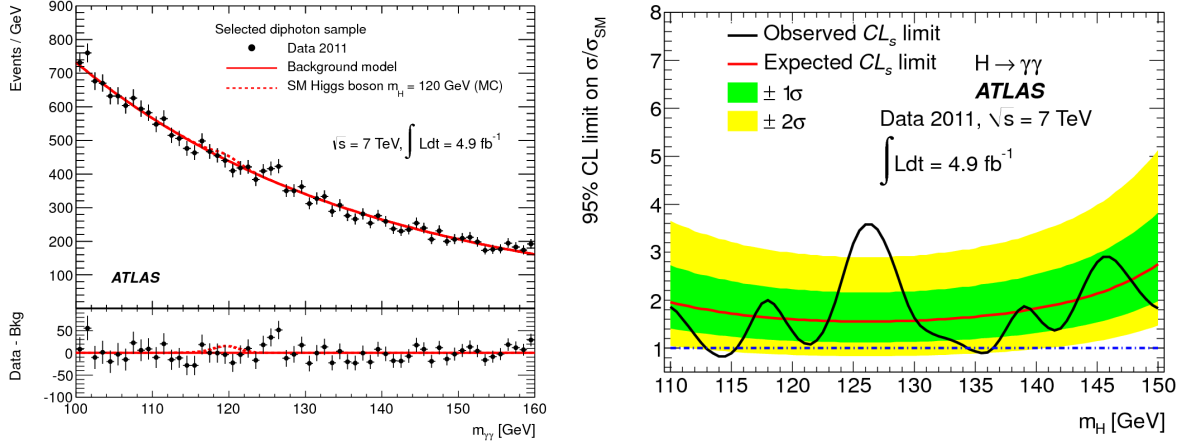


Figure 1: Left: Invariant diphoton mass distribution, overlaid with the total background from the fit to all sub-categories. The SM Higgs boson expectation for a mass hypothesis of 120 GeV is also shown. Right: Observed and expected 95% CL limits on the SM Higgs boson production in the $H \rightarrow \gamma\gamma$ decay channel normalized to the predicted SM cross section as a function of m_H .

3.2 $H \rightarrow \tau^+\tau^-$

The mass range from 100 GeV to 150 GeV can also be probed by the less sensitive $H \rightarrow \tau^+\tau^-$ decay channel with leptonic and hadronic decay modes of the two tau-leptons resulting in the fully-leptonic $\ell\ell 4\nu$, semi-leptonic $\ell\tau_{had}3\nu$ and fully-hadronic $\tau_{had}\tau_{had}2\nu$ final states. For an optimal analysis sensitivity, events are separated into 12 mutually exclusive sub-channels based on the lepton flavour and jet multiplicity, as well on the event topologies characteristic for the VBF and VH signal production mechanisms. The reconstructed mass shape of the dominant $Z \rightarrow \tau^+\tau^-$ background contribution is estimated by means of an embedding technique in which muons from Z decay events are substituted by simulated tau-lepton decays. The normalization of this background is obtained from the simulation. Background processes with jets misidentified as leptons or as tau-jets are estimated from the signal-free control data with reversed lepton isolation and tau-jet identification criteria, or samples with a same-sign charge of the two tau-lepton decay products. All other background contributions are estimated from simulation. Depending on the sub-channel the $\tau\tau$ invariant mass distribution used for the limit setting is reconstructed using the effective mass, collinear approximation or a Missing Mass Calculator [21] technique. The 95% CL exclusion limits on the SM Higgs boson production are shown in Figure 2. The observed limits vary from 2.5 to 11.9 times the predicted SM cross section over the entire explored mass range.

3.3 $VH, H \rightarrow b\bar{b}$

In order to suppress the extremely large multijet background contribution, the VH production mode is used to explore the $H \rightarrow b\bar{b}$ decay channel in the mass range from 100 GeV to 130 GeV. The search is divided into 11 sub-channels based on the decay mode of the associated vector boson and its transverse momentum: $\ell\nu b\bar{b}$ with four p_T^W bins, $\ell\ell b\bar{b}$ with four p_T^Z bins and $\nu\bar{\nu} b\bar{b}$ with three bins of the missing transverse energy. Since the Higgs and the vector boson tend to recoil away from each other, the highest sensitivity is reached in bins with highest transverse momenta of the vector bosons. The dominant background contributions originate from the Z +jets, W +jets, $t\bar{t}$, diboson and multijet processes. The shape of all but the last background process is obtained from the simulation, while the dedicated control data samples are used to estimate the shape of the multijet contribution and the normalization of all mentioned processes. The

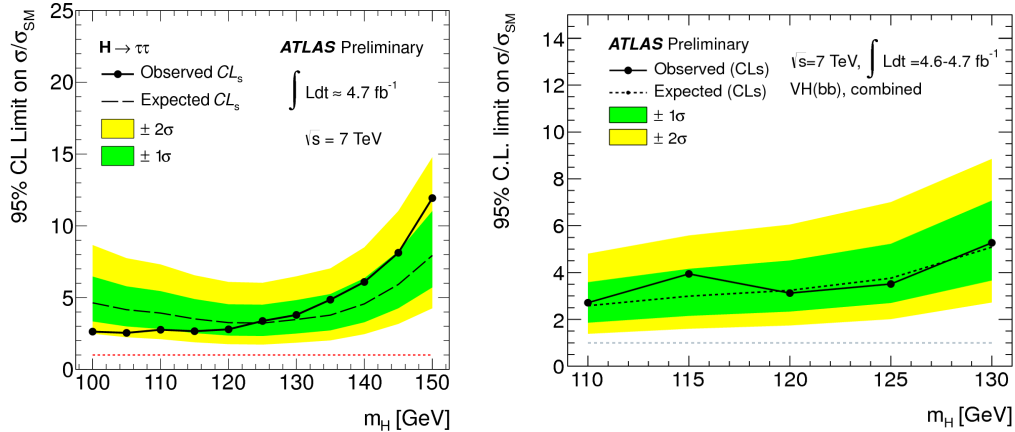


Figure 2: Observed and expected 95% CL limits on the SM Higgs boson production in the $H \rightarrow \tau^+\tau^-$ (left) and $H \rightarrow b\bar{b}$ (right) decay channels normalized to the predicted SM cross section as a function of m_H .

exclusion limits shown in Figure 2 are set based on the di- b -jet invariant mass distribution. The observed upper limits at the 95% CL on Higgs boson production vary from of 2.7 to 5.3 times the SM cross section in the entire mass range explored by this channel.

4 Searches in the high- m_H region (200 GeV - 600 GeV)

A high-mass Higgs boson will predominantly decay into a pair of vector bosons. Final states with a non-leptonic decay of one of the two vector boson have an advantage of a higher decay rate with respect to fully leptonic channels. At the same time, the background level can still be controlled using the invariant mass constraint of both vector bosons.

The $H \rightarrow ZZ \rightarrow \ell\nu\nu$ decay channel provides the highest sensitivity in the high- m_H region due to the high transverse momenta of leptons and neutrinos from the Z boson decays. The search is performed separately in $e\nu\nu$ and $\mu\mu\nu\nu$ sub-channels, both separated for low and high pile-up environment to account for the different resolution of the missing transverse energy. The invariant mass of the pair of the charged leptons is required to agree with the Z boson mass within 15 GeV. Different selection cuts are applied for searches below and above $m_H=280$ GeV, accounting for the different level of boost of the Z boson from the Higgs boson decay. The main background processes are suppressed mostly by the cuts on the opening angle of the two leptons from the Z boson decay and on the missing transverse energy. The contribution of the dominant ZZ background is estimated from simulation, while dedicated control data are used for other processes (WZ , $t\bar{t}$ and W/Z +jets). The transverse mass distribution is used for the limit setting. The observed (expected) exclusion limit at the 95% CL covers the mass range from 320 GeV to 560 GeV (260 GeV to 490 GeV), as shown in Figure 3 (left).

Somewhat lower sensitivity is reached in the $H \rightarrow ZZ \rightarrow \ell\ell jj$ channel which is divided into two sub-channels, one with maximum one jet tagged as a b -jet and one with two b -jets. Candidate events must have a lepton pair and a dijet pair with invariant masses compatible with the Z boson mass. The dominant $t\bar{t}$ and Z + jets backgrounds are suppressed by the cuts on the missing transverse energy and the opening angle between the two jets. The exclusion limit based on the $m_{\ell\ell jj}$ invariant mass distribution is shown in Figure 3 (right). Expected exclusion limit at the 95% CL covers the mass range from 360 GeV to 400 GeV, while the observed upper limit excludes the mass range from 300 GeV to 310 GeV and 360 GeV to 400 GeV.

The $H \rightarrow WW \rightarrow \ell\nu jj$ channel is separated into six sub-channels based on the lepton flavour and the jet multiplicity (0, 1 and 2 jets with a VBF-like topology). The invariant mass

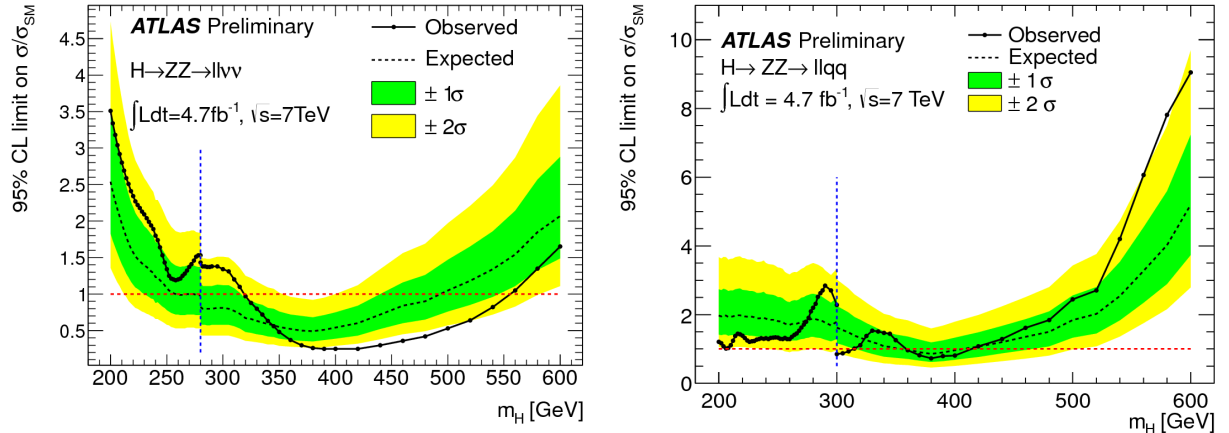


Figure 3: Observed and expected 95% CL limits on the SM Higgs boson production in the $H \rightarrow ZZ \rightarrow \ell\nu\nu$ (left) and $H \rightarrow ZZ \rightarrow \ell j j$ (right) decay channels normalized to the predicted SM cross section as a function of m_H .

of the dijet pair must be compatible with the W boson mass and a mass constraint $m_{\ell\nu} = m_W$ is applied to determine the z -component of the neutrino momentum. The limit setting is based on the resulting $m_{\ell\nu j j}$ invariant mass distribution. At present the channel is not sensitive enough to exclude the SM Higgs boson in the explored mass range from 300 GeV to 600 GeV at the 95% CL.

5 Searches in the full m_H region (110 GeV - 600 GeV)

The fully leptonic Higgs boson decays into two vector bosons provide a good handle for the background processes even in the case that one of the vector bosons is off-shell. These final states can therefore be used for the search in the entire mass range from 110 GeV to 600 GeV.

5.1 $H \rightarrow WW^{(*)} \rightarrow \ell\nu\ell\nu$

The Higgs boson search in the $H \rightarrow WW^{(*)} \rightarrow \ell\nu\ell\nu$ channel provides the highest sensitivity in a wide range of hypothesized Higgs boson masses. The analysis is divided in 9 sub-channels: $e\nu\nu$, $\mu\mu\nu\nu$ and $e\mu\nu\nu$, each separated by the jet multiplicity into final states with no jets, 1 jet or two jets with a VBF-like topology. The channel is characterized by a broad transverse mass distribution m_T for the Higgs signal due to the presence of two neutrinos in the final state. The main reducible backgrounds (W/Z +jets, multijets, $t\bar{t}$) are suppressed by the lepton isolation and b -jet veto requirement, as well as the cuts on the missing transverse energy. The dominant WW background contribution can be discriminated by means of topological cuts on the invariant dilepton mass and the opening angle between the two leptons. All background contributions remaining after the full selection are normalized using dedicated control regions and extrapolated to the signal region relying on predictions from the simulation. The transverse mass distribution is used in each sub-channel for the limit setting. As an example, the m_T distribution in the 0-jet sub-channel is shown in Figure 4 (left). The 95% CL exclusion limit with all sub-channels combined is shown in Figure 4 (right). No significant excess of events is observed. A SM Higgs boson with a mass in the range between 130 GeV and 260 GeV is excluded at the 95% CL, while the expected exclusion interval ranges from 127 GeV to 234 GeV.

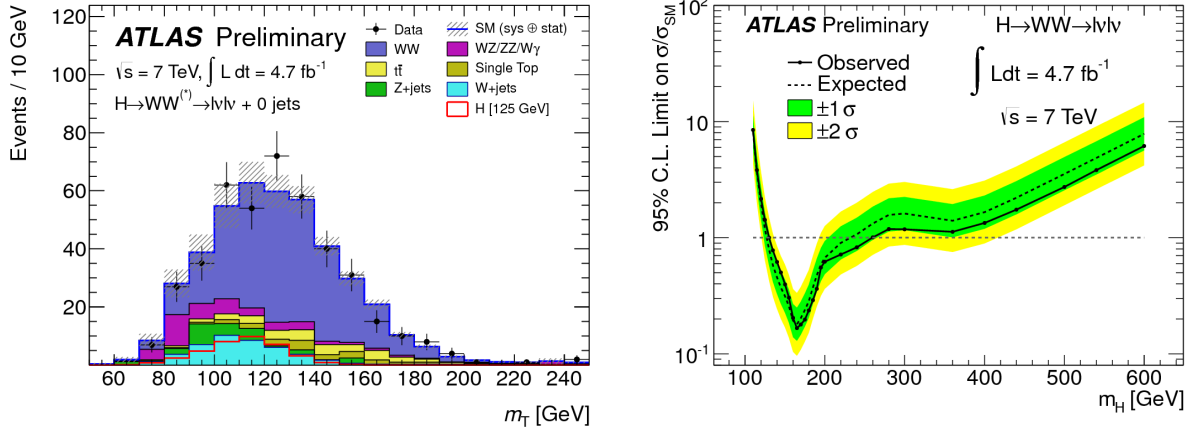


Figure 4: Left: Transverse mass distribution in the 0-jet $H \rightarrow WW^{(*)} \rightarrow \ell\nu\ell\nu$ sub-channel, compared to the background expectation. Right: Observed and expected 95% CL limits on the SM Higgs boson production in the same channel normalized to the predicted SM cross section as a function of m_H .

5.2 $H \rightarrow ZZ^{(*)} \rightarrow 4\ell$

The Higgs boson decays into four-leptons provide a clean signature with a very low level of background. After the lepton isolation and impact parameter cuts, the only remaining background for $m_H \gtrsim 200$ GeV is the irreducible ZZ process. For $m_H \lesssim 200$ GeV, there is a small additional contribution of the reducible $Zb\bar{b}$, Z +jet and $t\bar{t}$ backgrounds estimated from the control data samples. The channel is characterized by high experimental invariant mass resolution of 1.5% to 2% up to $m_H=350$ GeV, after which the natural Higgs boson decay width starts to dominate. A high signal efficiency is ensured by a high lepton reconstruction and identification efficiency, as well as the low transverse momentum cut of 7 GeV on the two subleading leptons. The mass of one dilepton pair is required to be compatible with the Z boson mass, while the m_H -dependent invariant mass cut is applied on the second lepton pair. The analysis is divided into four sub-channels based on lepton flavours: 4μ , $2e2\mu$, $2\mu 2e$ and $4e$, where the first two leptons are assigned to an on-shell Z boson. Figure 5 (left) shows the inclusive four-lepton invariant mass distribution after all selection cuts. A total of 62 ± 9 candidates are expected from background

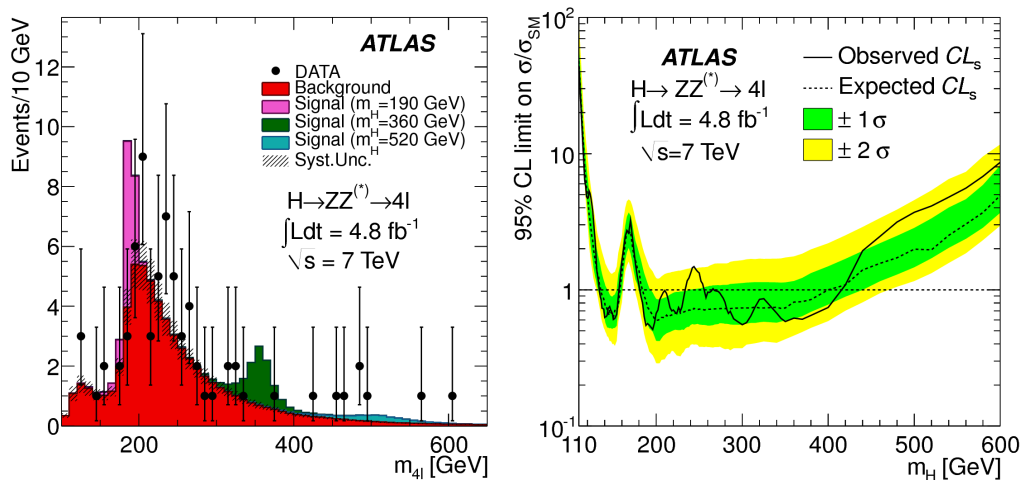


Figure 5: Left: Invariant four-lepton mass distribution of the selected candidates compared to the background expectation. Right: Observed and expected 95% CL limits on the SM Higgs boson production in the $H \rightarrow ZZ^{(*)} \rightarrow 4\ell$ decay channel normalized to the predicted SM cross section as a function of m_H .

processes which is in good agreement with 71 observed candidate events. The corresponding 95% CL exclusion limit is shown in Figure 5 (right). The observed exclusion covers the mass regions from 134 GeV to 156 GeV, 182 GeV to 233 GeV, 256 GeV to 265 GeV and 268 GeV to 415 GeV. The expected exclusion ranges are 136 GeV to 157 GeV and 184 GeV to 400 GeV. The most significant upward deviations from the background-only hypothesis are observed for $m_H = 125$ GeV with a local significance of 2.1σ , $m_H = 244$ GeV with a local significance of 2.2σ and $m_H = 500$ GeV with a local significance of 2.1σ . Once the look-elsewhere-effect is considered, none of the observed local excesses is significant.

6 Combined results

The results of the statistical combination of all individual search channels are summarized in Ref. [22]. The expected and observed limits obtained are shown in Figure 6. SM Higgs boson

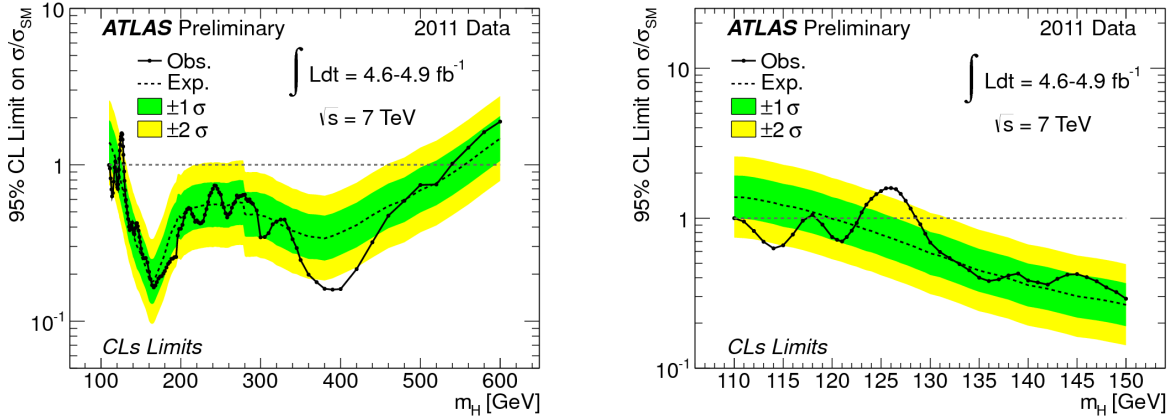


Figure 6: Combined observed and expected 95% CL limits on the SM Higgs boson production normalized to the predicted SM cross section as a function of m_H in the entire explored mass range (left) and zoomed in to the low-mass region (right).

masses between 120 GeV and 555 GeV are expected to be excluded at the 95% CL or higher. The observed 95% CL exclusion regions range from 110.0 GeV to 117.5 GeV, 118.5 GeV to 122.5 GeV, and 129 GeV to 539 GeV. The mass regions between 130 GeV and 486 GeV are excluded at the 99% CL.

The mass region around $m_H=126$ GeV cannot be excluded due to an observed excess of events compared to the expected background contribution. The p_0 -values in the given mass region are shown in Figure 7 for individual channels and their combination. The most significant excesses are observed in the two channels with high mass resolution, $H \rightarrow \gamma\gamma$ and $H \rightarrow ZZ^{(*)} \rightarrow 4\ell$. The largest combined local significance of the observed excess is 2.5σ , while the expected significance in the presence of a SM Higgs boson with $m_H=126$ GeV is 2.9σ . The global probability for such an excess to occur anywhere in the entire explored Higgs boson mass region from 110 GeV to 600 GeV is approximately 30%. The excess corresponds to the best-fit signal strength μ of approximately $0.9^{+0.4}_{-0.3}$, which is compatible with the signal strength expected from a SM Higgs boson at that mass, as shown in Figure 7 (right).

7 Summary

The full dataset of pp collision data recorded with the ATLAS detector at the LHC in 2011 has been studied in search for the SM Higgs boson, combining several Higgs boson decay channels

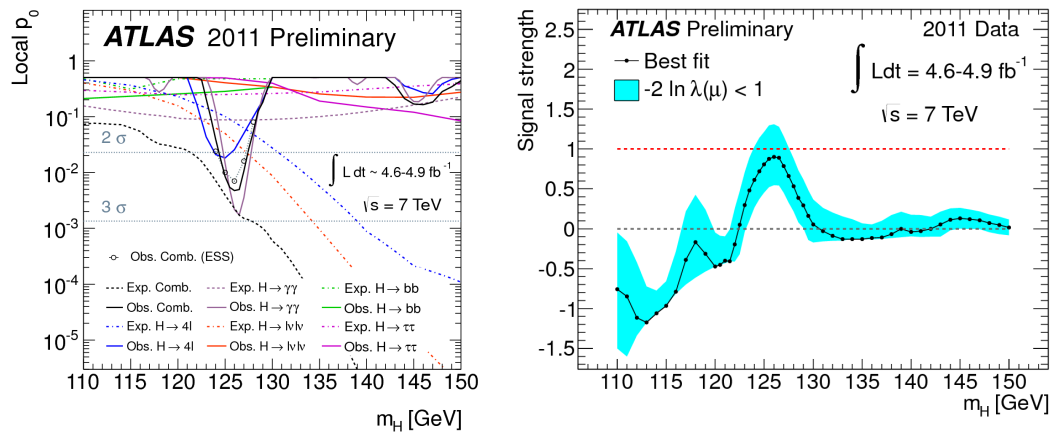


Figure 7: Left: The local p_0 -value for individual channels and the combination. The full curves give the observed individual and combined p_0 -value. The dashed curves show the median expected value under the hypothesis of a SM Higgs boson signal at that mass. Right: The best-fit signal strength $\mu = \sigma/\sigma_{SM}$ as a function of the Higgs boson mass hypothesis in the low mass range.

in the m_H range from 110 GeV to 600 GeV. A SM Higgs boson is excluded at the 95% CL in a wide mass range. The exclusion was not possible for m_H around 126 GeV, due to an observed excess of events at the local significance level of 2.5σ . More data collected in 2012 will be needed to better understand the origin of the described excess.

References

1. F. Englert, R. Brout, *Phys. Rev. Lett.* **13**, 321 (1964).
2. P. W. Higgs, *Phys. Lett. B* **12**, 132 (1964).
3. P. W. Higgs, *Phys. Rev. Lett.* **13**, 508 (1964).
4. G. S. Guralnik, C. R. Hagen, T. W. B. Kibble, *Phys. Rev. Lett.* **13**, 585 (1964).
5. LEP Electroweak Working Group, March 2012, <http://lepewwg.web.cern.ch/LEPEWWG/>.
6. R. Barate et al, *Phys. Lett. B* **31**, 565 (2003).
7. CDF and D0 Collaborations, arXiv:1203.3774.
8. ATLAS Collaboration, *Phys. Lett. B* **710**, 49 (2012).
9. ATLAS Collaboration, *Phys. Rev. Lett.* **108**, 111803 (2012).
10. ATLAS Collaboration, ATLAS-CONF-2012-014, <http://cdsweb.cern.ch/record/1429662>.
11. ATLAS Collaboration, ATLAS-CONF-2012-015, <http://cdsweb.cern.ch/record/1429664>.
12. ATLAS Collaboration, ATLAS-CONF-2012-012, <http://cdsweb.cern.ch/record/1429660>.
13. ATLAS Collaboration, *Phys. Lett. B* **710**, 383 (2012).
14. ATLAS Collaboration, ATLAS-CONF-2012-016, <http://cdsweb.cern.ch/record/1429665>.
15. ATLAS Collaboration, ATLAS-CONF-2012-017, <http://cdsweb.cern.ch/record/1429666>.
16. ATLAS Collaboration, ATLAS-CONF-2012-018, <http://cdsweb.cern.ch/record/1429667>.
17. A. L. Read, *J. Phys. G* **28**, 2693 (2012).
18. ATLAS and CMS Collaborations, LHC Higgs Combination Group, ATL-PHYS-PUB-2011-011, <https://cdsweb.cern.ch/record/1375842>.
19. LHC Higgs Cross Section Working Group, S. Dittmaier, C. Mariotti, G. Passarino, and R. Tanaka (Eds.), arXiv:1101.0593 [hep-ph].
20. E. Gross, O. Vitells, *Eur. Phys. J. C* **70**, 525 (2010).
21. A. Elagin, P. Murat, A. Pranko, and A. Safonov, *Nucl. Instrum. Methods* **654**, 481 (2011).
22. ATLAS Collaboration, ATLAS-CONF-2012-019, <http://cdsweb.cern.ch/record/1430033>.